JOURNAL OF PROPULSION AND POWER
Vol. 22, No. 4, July–August 2006

Pulse-Detonation-Engine Simulations with Alternative Geometries and Reaction Kinetics

X. He* and A. R. Karagozian†
University of California, Los Angeles, California 90095-1597

This paper describes numerical simulations, with simplified as well as full reaction kinetics, used to study a single-cycle pulse detonation engine (PDE) with alternative features. The focus of the present studies was on the influence of several characteristics of the PDE on performance and noise generation, including the presence of a nozzle extension at the end of the PDE tube, the influence of the complexity of the combustion reaction, and use of a quasi-one-dimensional simulation vs a full two-dimensional/axisymmetric simulation. Simplified reaction kinetics and quasi-one-dimensional simulations were in fact able to sufficiently capture important gasdynamic processes in the PDE as compared with complex reaction kinetics and two-dimensional/axisymmetric simulations; hence, reasonable estimates of engine performance could be made using simplified modeling. The presence of a divergent nozzle is seen to contribute to an overall increase in impulse for the PDE as compared with that for a straight nozzle, despite a resulting reduction in the differential pressure at the thrust wall. The presence of a convergent nozzle is seen to have the opposite effect, with a reduced overall impulse. There is also evidence that PDE tubes with a divergent nozzle can generate lower near-field sound pressure levels than the baseline configuration with a straight nozzle, suggesting the potential for optimization of PDE performance based on nozzle geometry.

Introduction and Background

THE pulse detonation engine (PDE) is a device that allows periodic ignition, propagation, and transmission of detonation waves within a detonation tube, with associated reflections of expansion and compression waves from the tube end, which can act in periodic fashion to produce thrust. The PDE concept holds promise for high thrust density in a constant-volume device requiring little or no rotating machinery. A number of groups have been exploring PDE tubes in recent years for propulsion applications.[1–10] This exploration has built on fundamental PDE studies over several decades, so that modern experimental diagnostic as well as computational methods can be used to bring about significant advances in the state of the art.

Performance parameters commonly used to characterize the pulse detonation engine include the impulse I, typically defined in terms of the temporal integral of pressure differential at the thrust wall $\Delta p_{\text{tw}}(t)$. When a nozzle is connected to the end of the straight PDE tube, it is necessary to account for the additional impulse arising from the contribution of pressure along the nozzle wall. In many cases this contribution to impulse from the nozzle can constitute a large portion of the total impulse. Hence the total impulse for the PDE takes the form

$$I \equiv A \int \Delta p_{\text{tw}}(t)\,\mathrm{d}t + \iiint \Delta p_{\text{noz}}(\sin\theta)\,\mathrm{d}A\,\mathrm{d}t \qquad (1)$$

where $\Delta p_{\text{noz}}(x, y, t)$ is the time-dependent pressure differential along the nozzle and $\mathrm{d}A$ is the area element of the nozzle interior surface, for example, oriented at an angle θ with respect to the axial direction. Nozzle symmetry produces an impulse contribution in the axial direction only. The impulse is usually scaled to produce the PDEs specific impulse $I_{\text{sp}} \equiv I/\rho V g$, in units of time, where ρ is the density of the reactive gas mixture in the tube, V is the detonation tube volume (including the nozzle volume, if it contains reactants), and g is the gravitational acceleration. I_{sp} is often used to compare performance among different PDE configurations and also to compare PDE performance with that of alternative engine cycles. The fuel specific impulse $I_{\text{sp},f} \equiv I_{\text{sp}}/Y_f$ is also commonly used for comparative purposes, where Y_f is the mass fraction of fuel in the reactants.

Overviews of past and ongoing numerical simulations of PDEs are described in recent papers by Kailasanath[3,4] and Kailasanath and Patnaik.[5] Other recent simulations have focused on various flow and geometrical features of the PDE, including the effects of nozzles placed downstream of the detonation tube. Cambier and Tegner[6] employ a second-order (total-variation-diminishing) (TVD) scheme in two dimensions and find that increasing the ratio of the nozzle exit area to the PDE tube area can produce monotonic increases in impulse I. Increasing the nozzle exit area is seen to cause a drop-off in I_{sp}; however, until $A_{\text{exit}}/A_{\text{tube}}$ reaches 4.0, because the nozzle volume (containing reactants) increases, but for area ratios large than 4.0, I_{sp} is seen to increase, suggesting that the impulse is increasing faster than the nozzle volume increases, per Eq. (1). In recent PDE experiments with nozzle extensions, Johnson[11] observes a decrease in the fuel specific impulse for converging-diverging nozzles as compared with straight nozzles or converging nozzles.

Modeling of partial fill and nozzle effects on PDEs by Cooper and Shepherd[12] makes use of the Gurney model[13] for the prediction of impulse from an explosive charge of reactants initially bounded by a tamper gas (which for the PDE consists of the inert gas in the nozzle or extension). Cooper and Shepherd find that, for a fixed energy associated with the gaseous explosive sandwiched between the thrust wall and the tamper gas, the I_{sp} scales as

$$I_{\text{sp}} \sim \frac{(N/C + 1/2)}{\sqrt{N/C + 1/3}} \qquad (2)$$

where N is the mass of the inert (within a nozzle or extension to the PDE) and C is the mass of the explosive material. This relation suggests that, for a fixed volume V of reactants and a fixed nozzle length, a divergent nozzle has the effect of increasing the impulse as compared with a straight nozzle, while a convergent nozzle has the effect of decreasing the impulse.

Presented as Paper 2004-469 at the AIAA 42nd Aerospace Sciences Meeting (parts were also presented at the 41st Aero Sci. meeting under paper 2003-1171, Reno, NV, 5–8 January 2004; received 24 May 2005; revision received 15 November 2005; accepted for publication 15 November 2005.

*Graduate Student Researcher, Mechanical and Aerospace Engineering Department; currently Postdoctoral Researcher, UCLA Department of Radiological Sciences, Los Angeles, CA 90095-1721.

†Professor, Mechanical and Aerospace Engineering Department; ark@seas.ucla.edu. Fellow AIAA.

Although these PDE nozzle tests have been conducted for single-cycle operation, for which scale-up to the multicycle performance is usually assumed, recent computations by Yungster[14] suggest that nozzle overexpansion during purge and filling processes might cancel any improvements in performance by the divergent nozzle itself. Nevertheless it is of interest to understand in a systematic manner the mechanisms whereby nozzles can increase or decrease PDE performance and in particular what the implications of the nozzle presence for pulse detonation engine noise levels may be.

Prior computation studies by our group pertaining to detonation phenomena[15] and to the pulse detonation engine in particular[16] involve both one- and two-dimensional simulations via high-order numerical schemes. Simulations of the single PDE cycle with simplified kinetics suggest that useful performance and noise-related estimates can be obtained even from one-dimensional computations of the straight pulse detonation engine tube.

The present studies focused on using these high-order schemes, both quasi-one-dimensional and two-dimensional, to study the behavior of the pulse detonation engine with a convergent, divergent, or straight nozzle connected to the PDE tube, using simplified as well as complex reaction kinetics. Special attention was focused on the detonation ignition processes, the influence of reactive kinetics and complexity, the validity of the quasi-one-dimensional approximation, and the influence of geometry on PDE performance parameters as well as pressure disturbances resulting in noise generation.

Problem Formulation and Numerical Methodology

The governing equations for the present simulations consist of the reactive Euler equations. For the simplified kinetics computations, a single species equation was solved (for reactant mass fraction Y), whereas for the simulations involving complex reaction kinetics, $N-1$ species equations were solved for the N species involved in the reactions. Full kinetics simulations of the stoichiometric combustion reactions for H_2–O_2 and H_2-air were considered here; the former mechanism contained eight species and 20 reactions,[17] whereas the latter mechanism contained 11 species and 23 elementary reactions and was part of the CHEMKIN II library.[18] The single step H_2-air mechanism was that of Ma et al.,[19,20] whereas the single step H_2–O_2 mechanism was derived from a fit to data obtained from a separate computation using STANJAN, as used in He and Karagozian.[16] A single-step CH_4–O_2 reaction was also employed in some of the computations,[16] in part because of the rapidity in required computational times for quick parametric studies, but also because of recent U.S. interest in exploring methane and oxygen as rocket propellants.

In the case where a nozzle extension was examined, both quasi-one-dimensional and full two-dimensional numerical simulations were performed to examine the influence of geometrical simplification in extracting PDE reactive flow processes. For example, Eq. 3 shows the governing equations for quasi-one-dimensional simulations of a PDE tube and nozzle of variable cross-sectional area $A(x)$ and with single-step reaction kinetics:

$$\frac{\partial}{\partial t}\boldsymbol{U}+\frac{\partial}{\partial x}\boldsymbol{F}=\frac{1}{A}\frac{\mathrm{d}A}{\mathrm{d}x}(\boldsymbol{H}-\boldsymbol{F})+\boldsymbol{S} \tag{3}$$

where the vectors containing conserved variables, flux terms, and the source terms are

$$\boldsymbol{U}=\begin{pmatrix}\rho\\ \rho u\\ E\\ \rho Y\end{pmatrix}\qquad \boldsymbol{F}=\begin{pmatrix}\rho u\\ \rho u^2+p\\ (E+p)u\\ \rho uY\end{pmatrix} \tag{4}$$

$$\boldsymbol{H}=\begin{pmatrix}0\\ p\\ 0\\ 0\end{pmatrix}\qquad \boldsymbol{S}=\begin{pmatrix}0\\ 0\\ 0\\ -K\rho Y e^{-(T_A/T)}\end{pmatrix} \tag{5}$$

Table 1 Values of constant terms in relations (5) and (6) for approximate single-step reactions

Reaction	q, J/kg	K	T_i, K
CH_4–O_2	1.0×10^7	3.224×10^8	24,000
H_2–air	2.72×10^6	7.5×10^9	13,000
H_2–O_2	1.344×10^7	3.224×10^8	24,000

Here ρ represents density, p is the static pressure, u is the x component of velocity, and γ is the ratio of specific heats. Here q is a heat-release parameter that characterizes the amount of energy released during the reaction, T_A represents the activation temperature, and K is the reaction-rate multiplier for the reaction source term. The heat-release term q is related to the total energy E through the relation

$$E=p/(\gamma-1)+\rho(u^2)/2+\rho qY \tag{6}$$

The values of the reaction-rate terms for the different single-step reactions explored in the present study are shown in Table 1.

In fully two-dimensional axisymmetric or planar simulations with a variable-area nozzle, governing equations in generalized coordinates were employed. Coordinate transformations and relevant eigenvectors were derived to allow the curved nozzle boundary to be transformed to and aligned with the computational grid.[17] Full two-dimensional simulations of the PDE with a variable-area nozzle and full reaction kinetics required computational times that were five to six times greater than for the quasi-one-dimensional simulations of the same PDE geometry but with simplified reaction kinetics.

The present simulations employed the weighted essentially nonoscillatory (WENO) scheme for spatial integration, which in benchmark tests[21,22] is claimed to be fifth-order accurate in smooth regions and third-order accurate in the vicinity of discontinuities. It is noted, however, per the recent analysis of Henrick et al.,[23] that in the vicinity of shock discontinuities WENO schemes might be only first-order accurate. For the single-step kinetics simulations, a third-order TVD Runge–Kutta method was used for time discretization. For full kinetics simulations, the method of operator splitting was used,[24] where the system of governing equations was split into separate sets of equations, one which only included the advection terms (solved via WENO) and one which only included reaction-rate source terms. A stiff ordinary differential equation (ODE) solver, DVODE (a variation of VODE[25]), was used for the solution of the rate equations; thermodynamic parameters and rate constants were obtained via the CHEMKIN II subroutine.[18] Parallelization of the code was also employed, whereby the computational domain was broken into four to eight sections and the computation within each section ran on separate nodes of a 16-node Beowulf cluster. Boundary information was passed between neighboring nodes using a standard message-passing-interface library.

The basic code was validated via extensive grid-resolution studies as described in prior work.[15–17] The degree of spatial resolution of the reaction zone can have a profound effect on the ability of the simulation to represent the detonation process accurately. For simulations of the canonical overdriven, pulsating detonation, a resolution of at least 20 grid points per detonation reaction zone half-length might be required.[15] Grid-resolution tests in the present and prior PDE simulations,[16] however, suggest that even five grid points per reaction zone half-length were sufficient for the cases under consideration.[17] In the present two-dimensional simulations, the grid spacing in the downstream dimension was 1 cm or less, while the grid size in the transverse direction was 0.3 cm. A Courant–Friedrichs–Lewy number of 0.1 was employed.

A computational "spark" adjacent to the thrust wall was used to initiate the detonation at the start of the PDE cycle. This narrow, high-pressure, high-temperature region was able to initiate a propagating shock and ignite the reactants; the flame front then caught up with the shock, forming a detonation. As suggested by prior studies,[5,8,26,27] however, such thermal initiation of detonation depends very strongly on the initial rate of deposition of energy in the reactants. This concept was validated in the present studies by

altering the initial temperature and pressure in the computational spark to be able to determine minimum input energy densities leading to detonation initiation.

In addition to the standard performance parameters used to characterize the PDE (I and I_{sp}), the local sound pressure level (SPL) at various locations within and external to the detonation tube was also computed. As done previously,[16] these were estimated by examining the Fourier transform of the time-dependent pressure measured at various locations within the computational domain. The SPL was then computed based on peak pressures in the Fourier spectrum for the standard relation $\mathrm{SPL} \equiv 20 \log_{10}(p/p_{\mathrm{ref}})$, where $p_{\mathrm{ref}} = 2 \times 10^{-5}$ Pa. This approach constitutes an estimate of the magnitude of local pressure disturbances as would be measured locally.

Yet prediction of far-field noise radiated to the surroundings by the pulse detonation engine, that is, beyond the present computational domain, is not as straightforward. Many commonly used methods for predicted supersonic jet noise, for example, make assumptions regarding the acoustic nature of the disturbances, for example, through Lighthill's analogy[28] or application of the Kirchoff integral formulation for aeroacoustic sources (as done in Eldredge[29]). The local pressure disturbances for the PDE are not acoustic, of course, and so application of any of these standard methods to the present problem is highly questionable. Separate studies were conducted[17] to examine approximations for pressure disturbances obtained using the Kirchhoff surface formulation as compared with "direct" computation of pressure disturbances using the present numerical schemes. These comparisons will be described.

Several different nozzle extension shapes were explored in the present study; these are shown in Fig. 1. The nozzle shapes included both convergent and divergent nozzles, in each case represented by a fifth-order polynomial shape. A straight "nozzle" extension was also examined as a baseline for comparison. In the present study on nozzles, the straight portion of the PDE tube, of length $L = 1$ m, was always assumed to be initially filled with reactants. The nozzle section of length $L_n = 1$ m was initially filled with inert gas at 1 atm and room temperature. For a single-step reaction, the inert consisted of products with mass fraction $(1 - Y)$, whereas for the complex reaction the inert consisted of air. In the simulations of straight PDE tubes without a nozzle, the tube was assumed to be initially filled completely with reactants. The effects of partial reactant fill on PDE performance have been explored by Li and Kailasanath,[30] Cooper and Shepherd,[12] and others, and scaling such as that indicated in Eq. (2) is observed.

For the fully two-dimensional simulations, the computational domain extended three PDE tube lengths beyond the end of the nozzle (or tube) extension and 10 PDE radii or widths away from the PDE centerline. In the quasi-one-dimensional simulations, the computational domain only extended a few grid cells beyond the end of the nozzle, and a zero pressure relaxation length (PRL) was employed. The effects of the pressure relaxation length on the accuracy of a one-dimensional PDE simulation have been explored in our prior work[16] and suggest that in many cases that a zero PRL can sufficiently represent PDE exit flow conditions, although Kailasanath and Patnaik[5] have identified conditions for which use of the PRL renders more accurate results.

Results

Validation: PDE Ignition and Baseline Performance Estimates

As already noted, the detonation process for the PDE was initiated by a computational spark represented by high-temperature and high-pressure gas adjacent to the thrust wall. This resulted in an effective internal energy, associated with the spark, which raised the local temperature and pressure of the reactants, generating a shock propagating away from the thrust wall and igniting the reactants.

The influence of the spar pressure and temperature (and resulting energy deposition) on initiation of a detonation wave, for validation purposes, was studied using the one-dimensional simulations with full kinetic mechanisms in a detonation tube initially filled with stoichiometric reactants. The high-pressure, high-temperature computational spark within the reactants, consisting of three grid cells adjacent to the thrust wall at the left of the domain, was used in these studies. Depending on the spark pressure and temperature, a shock wave that could ignite a Chapman–Jouguet (CJ) detonation could be initiated.

Figure 2, for example, indicates the evolution of the pressure distribution in a detonation tube initially filled with a stoichiometric hydrogen-oxygen-argon mixture. The computational spark (of initial pressure 3 atm and temperature 1500 K) was applied to the mixture of reactants, and the initially separated shock and reaction front quickly coalesced into a propagating detonation, with an asymptotic peak pressure near 18 atm. Other researchers have used computational sparks adjacent to the thrust wall to initiate the PDE cycle,[5,8] but these often involve using a narrow region of gaseous products at very high temperatures (above 3000 K) and pressures (above 30 atm), yielding asymptotic peak pressures for stoichiometric H_2–O_2–Ar near 25 atm. The present scheme explored a lower pressure and temperature spark region, applied to the reactant mixture, so as to be able to estimate critical input energies required to initiate detonations.

Figure 3 shows the centerline pressure distribution for a one-dimensional, full kinetics simulation of an H_2–O_2–Ar mixture, for different initial temperatures and pressures in the three grid cell-wide spark adjacent to the thrust wall. Critical combinations of temperature and pressure were observed to be necessary for the classical Zel'dovich-Von Neumann-Doering (ZND) detonation structure to evolve; if the initial energy deposition were too small, a weak shock front did not ignite the mixture and thus did not transition to a

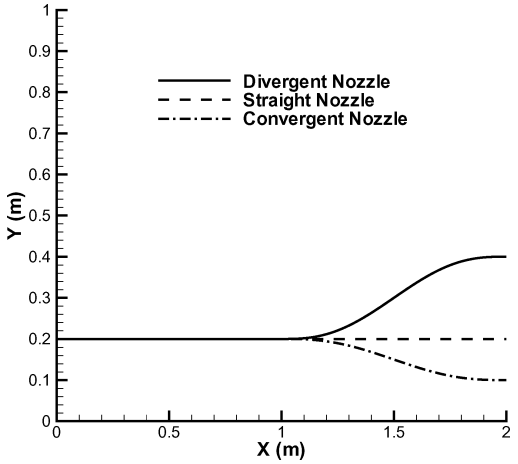

Fig. 1 Upper half of the different nozzle geometries explored in the present study. Reactants were initially at $X \leq 1$ m, while the nozzle itself (1 m $\leq X \leq$ 2 m) contained inert gas.

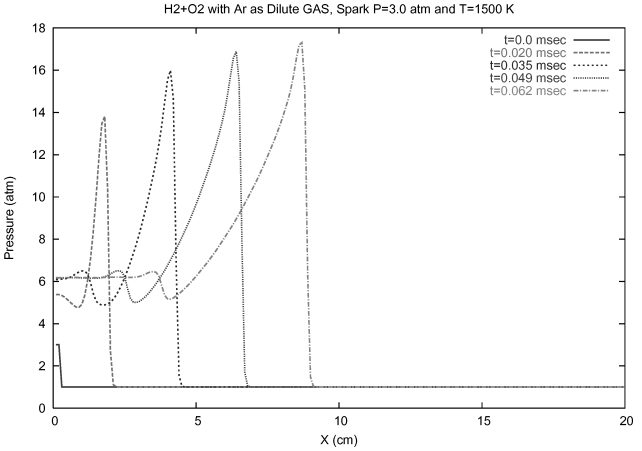

Fig. 2 Temporal evolution of the centerline pressure distribution for an H_2–O_2–Ar reaction with full kinetics, for a computational spark three grid cells in width with temperature 1500 K and pressure 3 atm.

Table 2 Initial temperatures, pressures, and input energies for a computational spark used to ignite an H_2–O_2–Ar mixture and determination of the possibility of detonation ignition

Temperature, K	Pressure, atm	Energy, erg/cm^2	Detonation?
500	3	2.02×10^5	No
1000	3	8.06×10^5	No
1500	3	9.95×10^5	Yes
2000	3	11.0×10^5	Yes
1500	5	15.3×10^5	Yes
1500	2.5	8.63×10^5	Yes
1500	2.0	7.3×10^5	No

Table 3 Initial temperatures, pressures, and input energies for a computational spark used to ignite an H_2–O_2–N_2 mixture and determination of the possibility of detonation ignition

Temperature, K	Pressure, atm	Energy, erg/cm^2	Detonation?
800	1	4.54×10^5	No
900	1	4.89×10^5	No
1000	1	5.18×10^5	Yes
1200	1	5.64×10^5	Yes

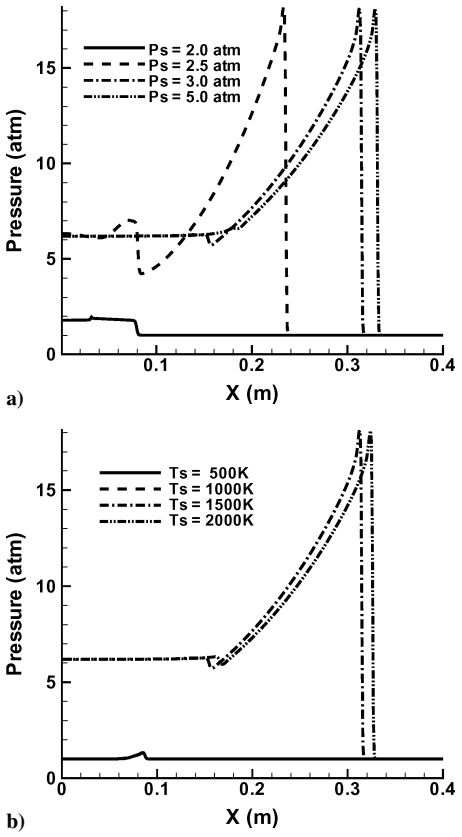

Fig. 3 Centerline pressure distribution for the H_2–O_2 reaction with full kinetics, for different computational spark conditions: a) fixed temperature 1500 K and variable pressure and b) fixed pressure 3 atm and variable temperature, each at time 0.2 ms.

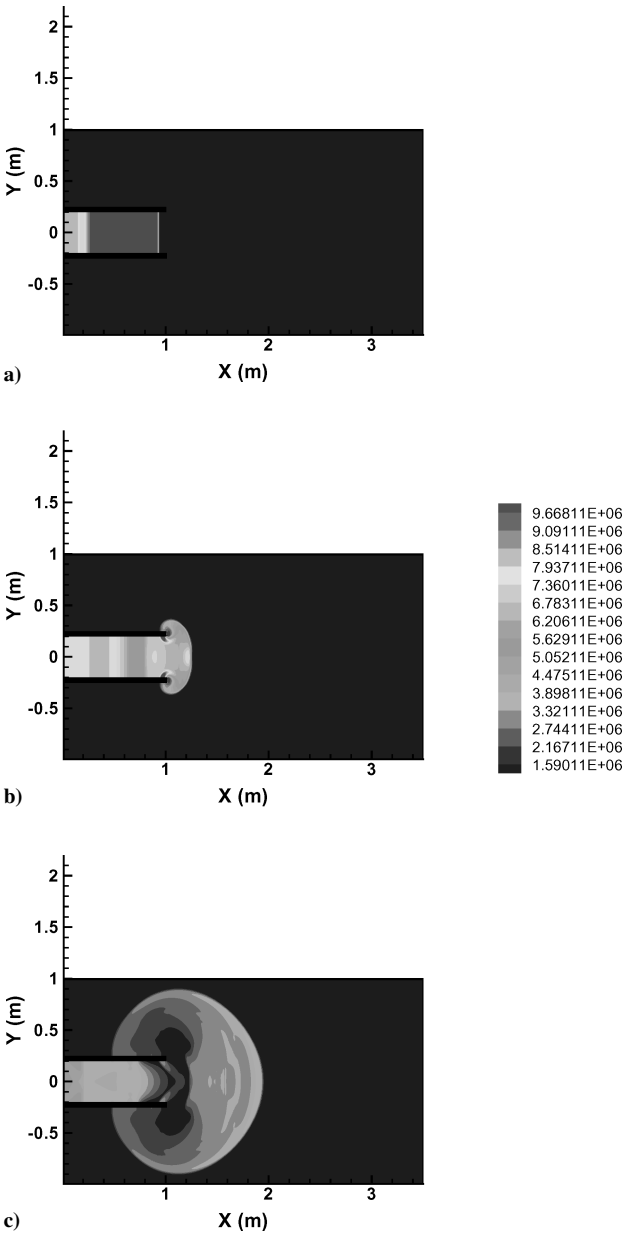

Fig. 4 Temporal evolution of the two-dimensional planar pressure field within and external to the PDE over one cycle, with pressure given in units of dyn/cm^2. Data shown are at times corresponding to a) 0.15 ms, b) 0.47 ms, and c) 1.34 ms. A H_2–O_2 reaction was simulated here with full chemical kinetics.

detonation, as seen by the solid lines in Figs. 3a and 3b. Tables 2 and 3, for H_2–O_2–Ar and H_2-air reactions, respectively, quantify the conditions that were required for ignition of a detonation.

As expected, the critical input energies for ignition of a detonation were found to be different for these different reactions. In the case of H_2-air, a critical energy deposition per unit area of about 5×10^5 erg/cm^2 was required for detonation, whereas for the case of H_2–O_2–Ar this critical value rose to about 8.5×10^5 erg/cm^2. Although there are not extensive quantifications of required detonation ignition energies for comparison here, Benedick et al.[31] suggest that a stoichiometric H_2-air mixture has a detonation ignition energy of approximately 8.0×10^5 erg/cm^2, which is well within the range estimated by the present computations. The spark pressures and temperatures indicated in Tables 2 and 3 were found to be of the same magnitude as those utilized by Kailasanath and coworkers[5,30] for PDE ignition, but were considerably smaller than those required for detonation ignition in the computational study by Ebrahimi and Merkle,[8] for example. These latter studies employ a relatively large spark region, however, where a reflected expansion from the closed PDE tube end can weaken the downstream propagating shock before combustion is initiated. In the present PDE studies, sufficiently high spark energies were selected for the small spark region to ensure rapid initiation of a detonation.

Following these preliminary ignition estimates, full kinetics simulations of the reactant-filled, straight PDE tube without a nozzle allowed a detailed examination of the detonation ignition and propagation process to be made, in addition to quantitative comparisons with experimental data. Figure 4 displays the evolution of the two-dimensional pressure field associated with the PDE tube and

its surroundings, for a full H_2–O_2 reaction. As seen in prior two-dimensional simulations of the PDE but with simplified kinetics,[16] the propagation of the detonation out of the tube resulted in the propagation of a vortical structure coincident with the shock and simultaneous reflection of an expansion fan back into the tube.

The temporal evolution of the pressure distribution along the centerline of the straight PDE tube is shown in Figs. 5 and 6 for a two-dimensional axisymmetric configuration with complex and simplified H_2-air reaction kinetics, respectively. Here the propagation of the detonation wave through the PDE tube (a) and the exit of the shock from the tube and reflection of the expansion fan from the exhaust back into the tube (b and c) are more clearly visible. These observed centerline pressure profiles were quantitatively quite similar between the complex and simplified reaction kinetics cases throughout the course of the PDE cycle. Even examinations comparing the evolution of the mass fraction of products (H_2O)

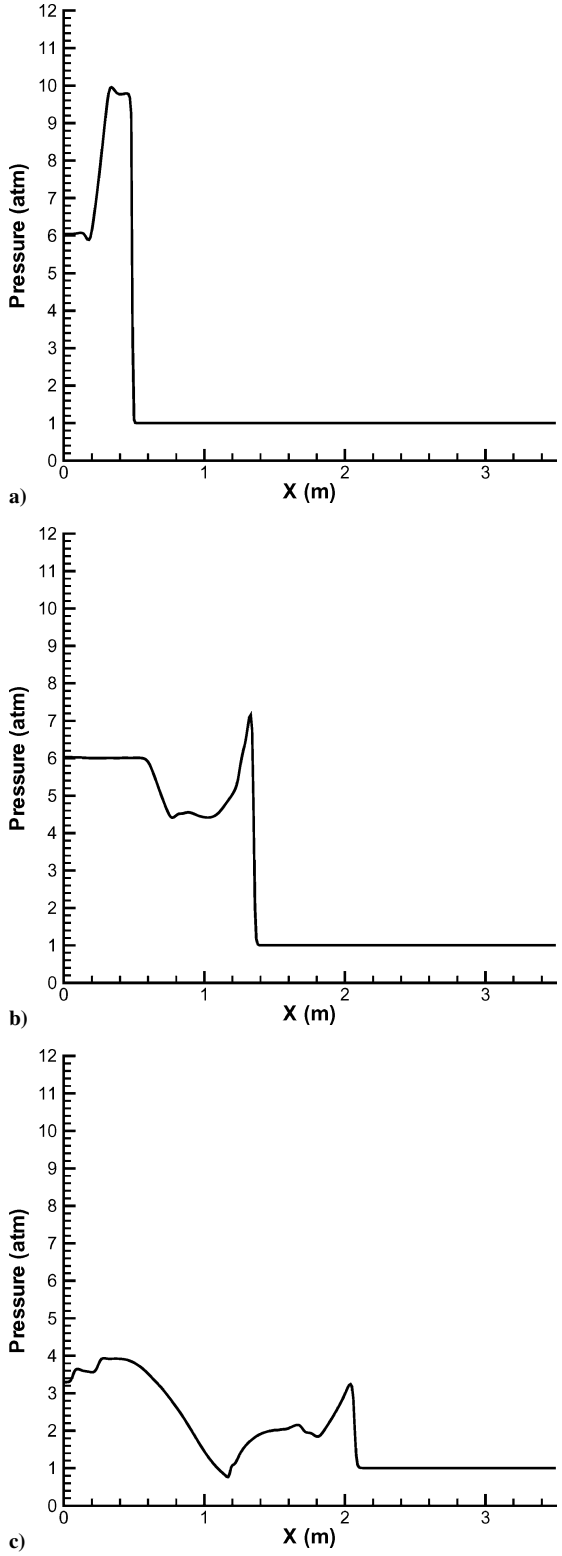

Fig. 5 Evolution of the centerline pressure for a straight two-dimensional axisymmetric PDE of 1 m length, for full H_2-air reaction kinetics, at times a) 0.20 ms, b) 0.81 ms, and c) 1.8 ms.

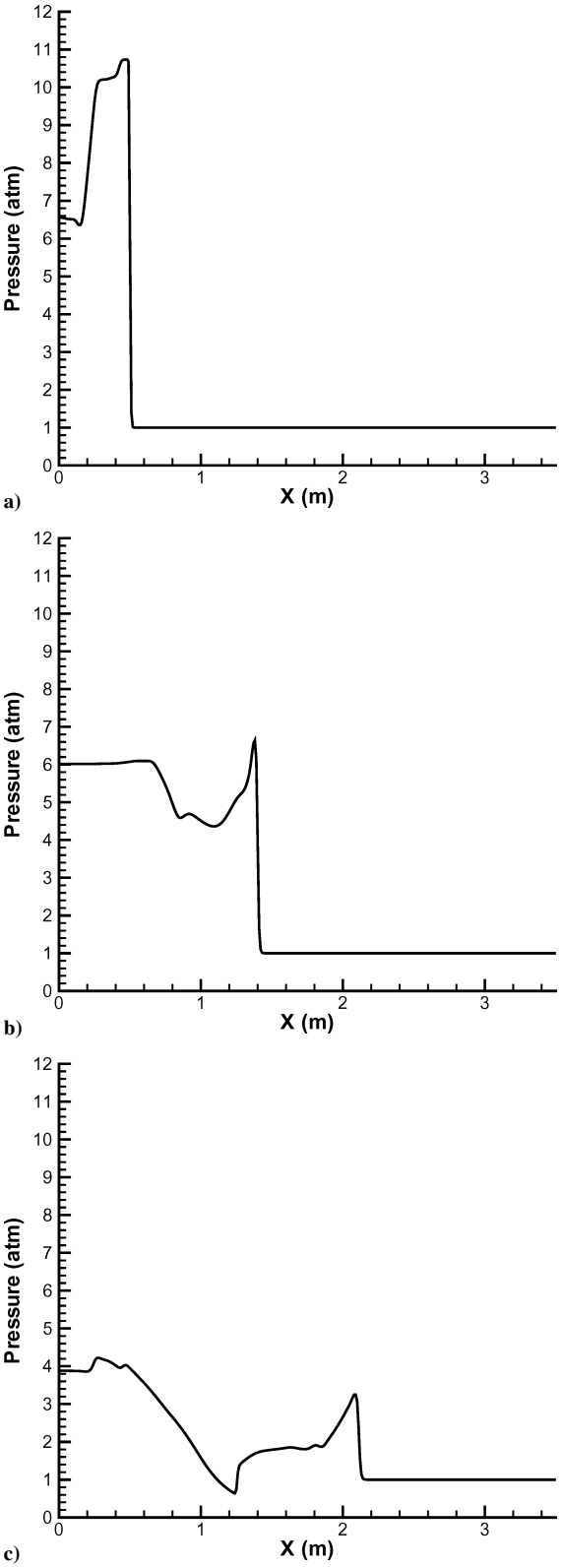

Fig. 6 Evolution of the centerline pressure for a straight two-dimensional axisymmetric PDE of 1 m length, for single-step H_2-air reaction kinetics, at times a) 0.19 ms, b) 0.81 ms, and c) 1.7 ms.

Table 4 Comparison of specific impulse for single-cycle straight PDE tube between the present simulations and corresponding studies, as noted

Study	I_{sp}, H_2-air, s	I_{sp}, H_2–O_2, s
Present (full kin.)	128.5	240
Present (simpl. kin.)	122	230
Wintenberger et al.[7]	142	189
CIT expts.[7]	——	200
Ebrahimi and Merkle[8]	——	252
Zitoun and Desbordes[32]	149	226
Schauer expts.[33]	113	——

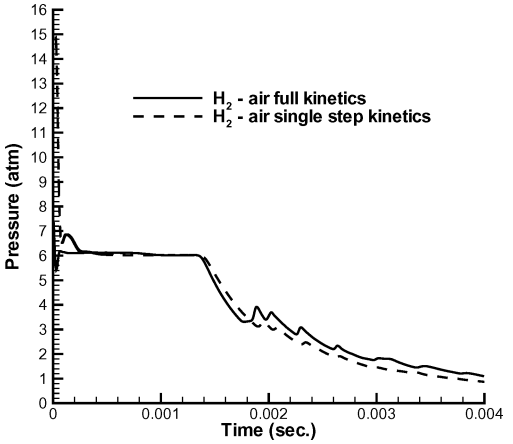

Fig. 7 Temporal evolution of the pressure at the thrust wall for a straight two-dimensional axisymmetric PDE of 1 m length, for full and single-step H_2-air reaction kinetics.

between full and simplified kinetics yielded very small differences over a single cycle, at most around 5% throughout the cycle.[17] The simplified scheme's reaction timescales were thus sufficient to be able to represent critical PDE thermodynamic processes, as will be discussed further.

For this straight PDE tube simulation (without a nozzle), the pressure evolution at the thrust wall was the only contributor to the PDE impulse. A similar temporal pressure evolution at the thrust wall emerged between full and simplified kinetics simulations (see Fig. 7), which in turn produced similar values of the asymptotic values of impulse I and specific impulse I_{sp}. In the present computations, the impulse [Eq. (1)] was integrated numerically over time until the pressure at the thrust wall dropped to ambient (atmospheric) conditions. Various I_{sp} values for the hydrogen-air as well as the hydrogen-oxygen simulations extracted from results such as those in Fig. 7 are shown in Table 4. Comparisons with I_{sp} quantified from others' PDE experiments and simulations are also shown, indicating reasonable agreement with established values. The simplified reaction mechanisms for H_2-air and $H_2 - O_2$ reactions employed in the present study appeared to reasonably predict the pressure evolution in the PDE cycle. The lack of a short-lived pressure spike and a slightly slower decay in pressure at the thrust wall predicted by the full kinetics simulations resulted in slightly higher I_{sp} values.

Pressure Disturbances and Noise Estimates

Time-series pressure data were used to estimate the sound pressure level present at various locations in the flowfield over a single PDE cycle. As noted earlier, a Fourier transform of the pressure signal at various locations allowed estimates of the peak sound pressure level, for example, for the two-dimensional simulations of the straight PDE tube with a hydrogen-air reaction. In most locations for this case, we observed the peak in pressure to appear close to the frequency associated with the period of the PDE cycle, which would be expected for data extracted from a single period. The resulting rough estimates of SPL at various locations are quantified in Table 5. Although the estimates of the pressure disturbances here were approximate, there was reasonable correspondence with experimental sound-pressure-level measurements made in roughly the same location for 1-m PDE tubes operating with stoichiometric H_2-air mixtures at the Air Force Research Lab at Wright–Patterson Air Force Base.[34]

Table 5 Computed sound pressure level at various locations within the tube (thrust wall, center of tube) and at one-half a PDE tube length downstream of the tube end (Results are obtained from two-dimensional axisymmetric simulations.)

Study	Thrust wall, dB	Midtube, dB	Downstream, dB
Present, H_2 air (full kin.)	208	207	192
Present, H_2 air (simpl. kin.)	209	208	192
Expts., Schauer and Shaw (personal communication)	——	——	192 (approx)

This method for estimating local sound pressure level allowed the flowfield throughout the computational domain to influence the pressure field, and hence the local disturbance, at a given location. Several alternatives are typically available for estimates of noise, but to estimate the actual noise generated by the PDE, especially the far-field noise radiating beyond the computational domain, only very rough approximations were possible. The Kirchhoff surface method,[29,35] for example, is that by which important information regarding a sound source, including its nonlinear effects, is typically captured within a designated surface surrounding the source. This approach was explored as a possible alternative method to local pressure determinations via full numerical solution in He.[17] The method allows radiating sound from the source to be evaluated based on quantities (pressure, etc.) evaluated on this surface as long as the wave equation (and hence acoustic disturbances) are valid outside of the surface. The PDE flowfield, involving detonations and shocks, clearly does not have acoustic disturbances in the vicinity of the device and its exterior, and thus alternatively sized Kirchhoff surfaces within the present domain of computation still violated the fundamental assumption of exterior acoustic disturbances. Accordingly, estimates of pressure disturbance amplitudes and wave speeds within the computational domain (but outside of the estimated Kirchhoff surface) were found to differ considerably from estimates made by the preceding direct computational method. Lighthill's acoustic analogy[28] was similarly found to be inappropriate for application for the present problem. Hence the present method for determining local SPL, although clearly approximate, was deemed the most appropriate for the given computational domain and PDE size.

Yet the present SPL estimates, based on direct computation of local pressure disturbances, did suggest that noise in the near- to midfield region of the PDE tube could be estimated and its decay scaled with respect to distance from the PDE exit. For example, the peak pressure along the centerline of the PDE (extracted from the two-dimensional axisymmetric simulations and Fourier transform of the time-dependent pressure measured at various locations) appeared to scale with distance r from the exit of the PDE as

$$(p/p_{\text{ref}}) = C/(r/D)^k \qquad r \geq L \tag{7}$$

where D is the diameter of the straight PDE tube. For the case with $L = 1$ m, $D = 0.4$ m, and for the CH_4–O_2 reaction, for example, C is equal to 7.32×10^9 and $k = 0.727$. This scaling suggested, for example, that the local SPL could drop from 191 dB near the PDE tube exit to about 177 dB at a distance 10 tube lengths downstream of the tube. The pressure decay suggested in Eq. (7) is of a similar format to that of the blast-wave decay theory of Sedov–Taylor,[36] except with a smaller exponent k than is usual. This likely means that the present simulation was not conducted far enough downstream to be able to precisely extract this type of self-similar solution.

Nozzle Effects and Quasi-One-Dimensional Simulations

Our prior studies[16] demonstrate that a one-dimensional simulation of the straight PDE tube quantitatively yields a very similar pressure field evolution to that of the two-dimensional simulation, even without inclusion of a one-dimensional PRL downstream of

the exit, over which the pressure is reduced linearly to atmospheric. This observation can depend on the specific PDE configuration, reaction process, and operating conditions, however.[5] In the present study it was of interest to determine if a quasi-one-dimensional simulation of PDE performance with a divergent or convergent nozzle could replicate the performance parameters quantified using fully two-dimensional simulations. In all nozzle test cases the PDE tube itself was assumed to be filled with a stoichiometric mixture of reactants, while the nozzle was assumed to be filled with inert (air for the full kinetics simulations and products for the single-step reaction kinetics simulations). The presence of an interface between the reactants and the inert can significantly diminish the strength of the propagating detonation wave/shock. The reduced strength of the propagating detonation and earlier reflection of a weak expansion wave then can produce a corresponding reduction in the overall cycle impulse. Thus in our employing a reactant-filled PDE tube with an inert-filled nozzle extension, the relative influences of nozzle shapes should impact primarily the strength of the propagating shock wave through the nozzle.

Figures 8, 9, and 10 show the temporal pressure evolution at various locations within the tube and nozzle for the straight, divergent, and convergent nozzles, respectively. The CH_4–O_2 single-step reaction was employed in these simulations. In most instances, the quasi-one-dimensional simulation replicated the far more complex two-dimensional axisymmetric simulation very well. The major differences that did arise between the quasi-one-dimensional and the two-dimensional simulations were all in the vicinity of the nozzle exit (Figs. 8c, 9c, and 10c). Because the quasi-one-dimensional simulations did not include a pressure relaxation length, a much more abrupt pressure drop occurred at the nozzle exit than in the full axisymmetric simulations. Although this comparison could be remedied with the inclusion of a PRL, the performance parameters and SPL values derived from quasi-one- and two-dimensional simulations were sufficiently close that the added parameter was not necessary, as is discussed next.

Figures 11 and 12 show differences in impulse produced by these different nozzle geometries (convergent, divergent, and straight). Figure 11 plots the contribution to the impulse that comes only from the pressure differential at the thrust wall, and based on the preceding results there is little difference between impulses predicted by the quasi-one- and two-dimensional simulations. Figure 12 shows the total impulse over time for the PDE with the nozzle extensions, where contributions from the pressure differential at the thrust wall as well as the nozzle shape were taken into account. Clearly there was a positive contribution to overall PDE impulse for a divergent nozzle as compared with the straight nozzle and a relative negative contribution to impulse for a convergent nozzle, caused by component forces acting in the downstream axial direction at the nozzle surface. These trends have also been observed, for example, by Falempin et al.,[37] who studied experimentally the effects of nozzles on PDE performance. In contrast, the results in Fig. 11 show that the contribution to impulse from the thrust wall pressure only was reduced for the divergent nozzle relative to that from the straight nozzle, whereas that for the convergent nozzle was increased. The divergent nozzle appeared to produce a reflected expansion wave (at both the tube-nozzle interface and the nozzle exit) with a greater pressure drop than did that reflected by the other nozzles, and the opposite occurred for the convergent nozzle. This larger pressure drop as a result of continuous reflected expansion waves generated by the interface at a divergent nozzle was also observed by Cooper and Shepherd.[12]

Hence a "competition" between the contribution to impulse from the thrust wall and the nozzle shape was seen to manifest itself. In principle a specific (lower weight) convergent nozzle shape could lead to an overall increase in impulse as a result of the increase in thrust wall pressure, or alternatively, as seen in the present example, the (higher weight) divergent nozzle's geometry could overcome the reduction in thrust wall pressure to produce overall a higher PDE impulse. The results in Fig. 12 suggest that the quasi-one-dimensional representation of the nozzle with simplified reaction kinetics was able to capture sufficiently accurately the overall flow processes and performance of the PDEs with a nozzle, making this a useful tool for studying this optimization.

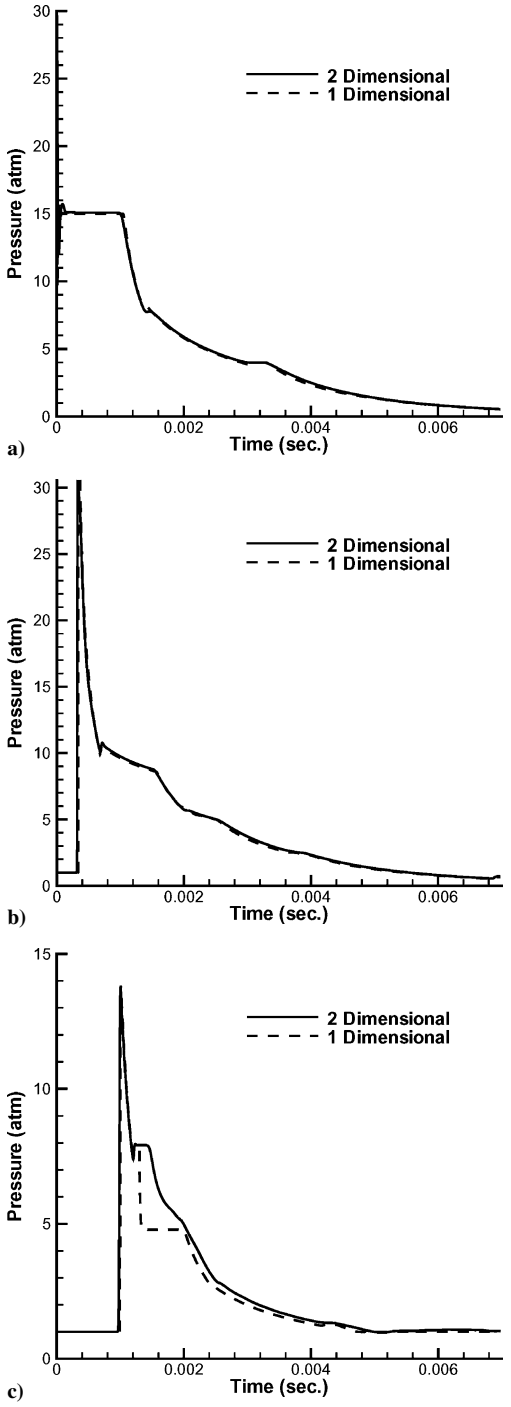

Fig. 8 Temporal evolution of the pressure at various locations in the PDE with a straight nozzle, for both quasi-one- and two-dimensional simulations with the CH_4–O_2 single-step mechanism. Results are shown for locations a) at the thrust wall, b) at the end of the straight PDE tube, and c) at the end of the nozzle extension.

Even simple models for PDE behavior and the influence of the inert-filled nozzle, for example, that based on Gurney,[12,13] can be useful in predicting trends, say, in lieu of the simulation results shown in Fig. 12. Although the predictions using Eq. 2 indicate that the impulse for the divergent nozzle should be about 14% greater than for the straight nozzle, the two-dimensional simulation results indicate about a 5% increase. The decrease in impulse predicted for a convergent model using the Gurney model in Eq. (2) is about 8%, in contrast to a 4% decrease from the full two-dimensional simulation at the end of the cycle. These predictions are not unreasonable,

Table 6 Computed sound pressure level, in decibels, for the three difference nozzle extensions (convergent, straight, divergent) at various locations within the PDE tube, nozzle, and flowfield exterior to the device[a]

Nozzle	(a) 2D[b]	(a) 1D[c]	(b) 2D	(b) 1D	(c) 2D	(c) 1D	(d) 2D	(d) 1D	(e) 2D	(f) 2D
Conv.	208.6	208.6	206.3	206.4	203.8	203.7	199.0	198.3	191.5	186.2
Str.	209.6	209.7	207.0	207.2	203.6	203.3	198.7	197.3	192.3	190.6
Div.	209.6	209.5	205.8	205.8	200.9	200.0	197.6	193.6	190.4	189.2

[a]Locations shown, with reference to Fig. 1, are as follows: (a) thrust wall center ($X = 0$ m, $Y = 0$ m), (b) tube end/nozzle start ($X = 1$ m, Y = 0 m), (c) nozzle midpoint ($X = 1.5$ m, $Y = 0$ m), (d) nozzle end ($X = 2.0$ m, $Y = 0$ m), (e) beyond the nozzle exit ($X = 3.0$ m, $Y = 0$ m), and (f) beyond the nozzle exit and above the exit ($X = 3.0$ m, $Y = 0.8$ m). Results are obtained from two-dimensional axisymmetric simulations with a simplified methane-oxygen reaction. Note that the quasi-one-dimensional simulation did not extend beyond the nozzle exit; hence, there were no one-dimensional data for comparison with the two-dimensional predictions at points (e) and (f).
[b]2D = two dimensional. [c]1D = one dimensional.

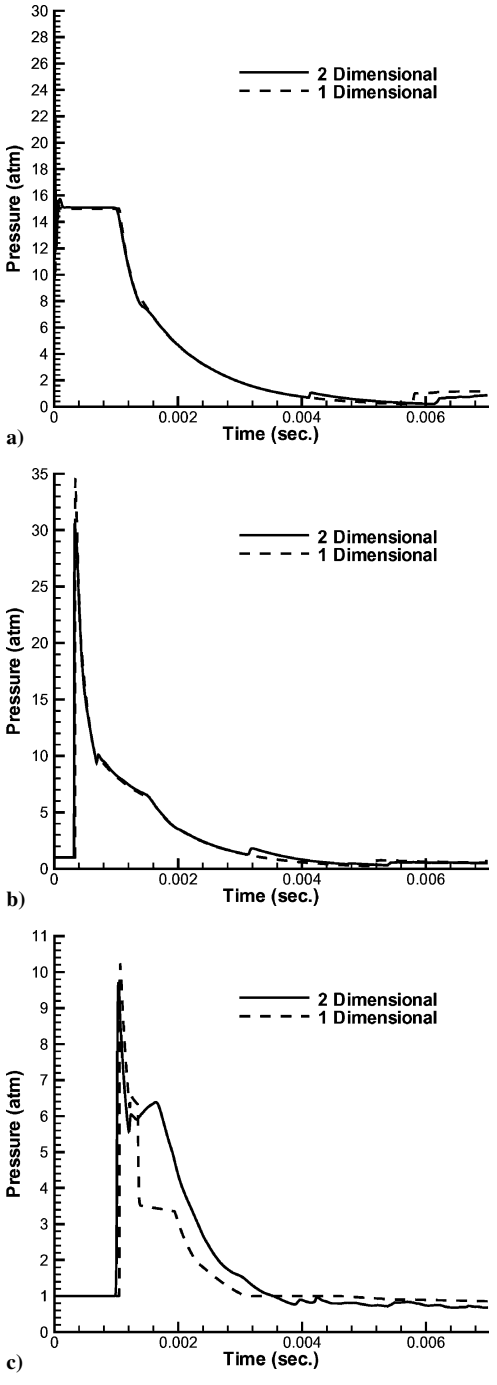

Fig. 9 Temporal evolution of the pressure at various locations in the PDE with a divergent nozzle, for both quasi-one- and two-dimensional simulations with the CH_4–O_2 single-step mechanism. Results are shown for locations a) at the thrust wall, b) at the end of the straight PDE tube, and c) at the end of the nozzle extension.

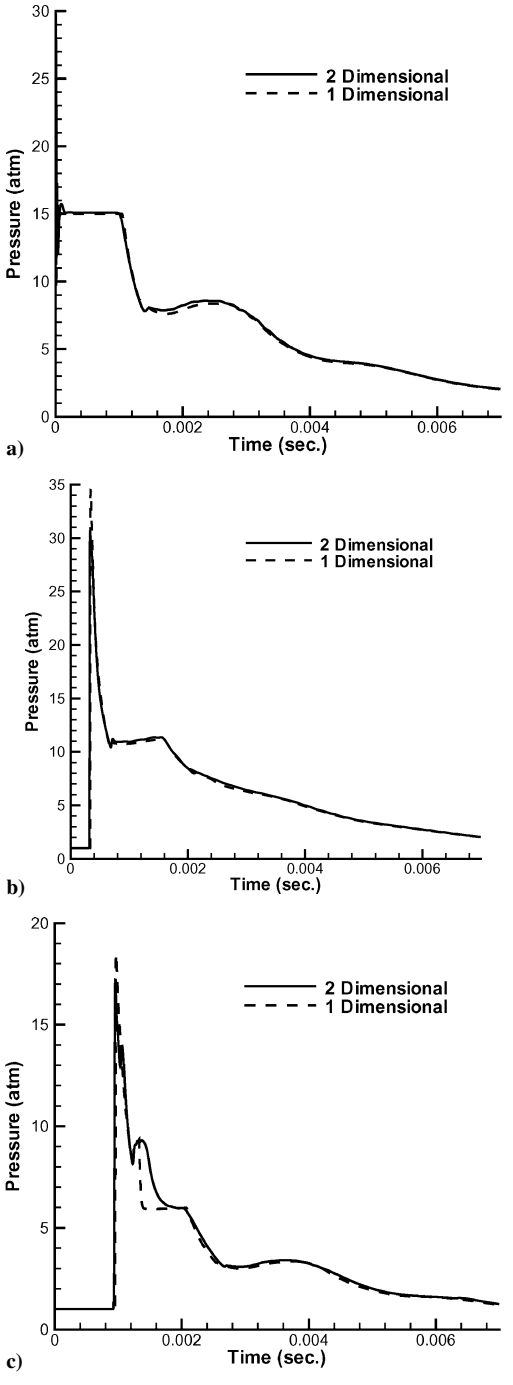

Fig. 10 Temporal evolution of the pressure at various locations in the PDE with a convergent nozzle, for both quasi-one- and two-dimensional simulations with the CH_4–O_2 single-step mechanism. Results are shown for locations a) at the thrust wall, b) at the end of the straight PDE tube, and c) at the end of the nozzle extension.

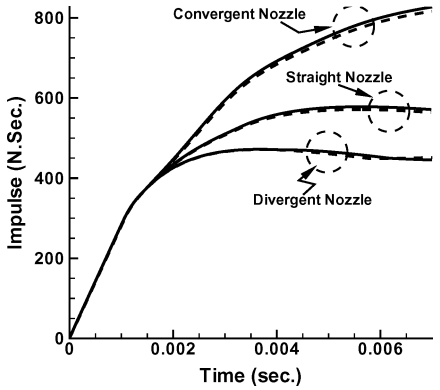

Fig. 11 Comparison of the evolution of the PDE impulse, based only on the thrust wall pressure differential, with time for quasi-one-dimensional simulations (- - - -) and full two-dimensional simulations (———) with simplified CH_4–O_2 kinetics. Divergent, convergent, and straight nozzle extensions are presented.

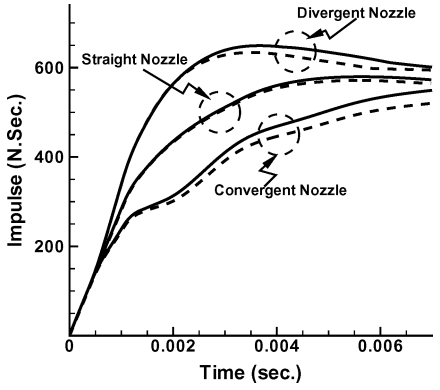

Fig. 12 Comparison of the evolution of the total PDE impulse with time for quasi-one-dimensional simulations (- - - - -) and full two-dimensional simulations (———) with simplified CH_4–O_2 kinetics. Divergent, convergent, and straight nozzle extensions are presented.

especially considering the relative simplicity of the model in comparison to either quasi-one or two-dimensional simulations.

Interestingly, in predicting sound pressure levels generated by the PDE with the nozzle extension, there was similarly little difference between the two-dimensional and quasi-one-dimensional predictions. Table 6 displays the simulated results for sound pressure level at various locations (with reference to locations within and external to the PDE nozzle indicated in Fig. 1). Within the PDE tube and nozzle (locations a–c), there was no appreciable difference between two-dimensional and quasi-one-dimensional predictions of SPL, whereas at the nozzle exit (location d) there was a slight difference for the divergent nozzle, consistent with differences in the pressure evolution at the nozzle exit (Fig. 9b). Exterior to the nozzle, along the PDE centerline (location e), the divergent nozzle SPL was slightly lower than that for the other nozzles, but not significantly so. This suggests that divergent nozzles might have a benefit for PDEs both in terms of increased performance and reduced noise generation, but these benefits will clearly depend on specific geometries.

Conclusions

The present simulations suggest that a great deal of useful performance and noise-related data can be obtained even from quasi-one-dimensional computations of the pulse detonation engine with simplified reaction kinetics. The present simulations were observed to provide robust, accurate simulations of the reactive and nonreactive flow processes occurring within the PDE. Very similar centerline pressure profiles were observed when comparing complex and simplified reaction kinetics simulations throughout the course of the PDE cycle, suggesting that the inclusion of appropriate reaction timescales in a simplified mechanism could be sufficient to be able to represent critical PDE thermodynamic processes, including local pressure disturbances, and ultimately, noise generation. Scaling of peak pressure data with downstream distance suggested that significant reductions in sound pressure level, of the order of 15 dB over 10 tube lengths, could occur beyond the PDE tube end.

Comparisons of PDE tube performance with differently shaped nozzle extensions yielded very interesting results. Not only were quasi-one-dimensional simulations with simplified kinetics able to capture flow and reaction processes reasonably well as compared with a full two-dimensional axisymmetric simulation, the optimization of the influence of the nozzle on performance and noise could also be studied in a straightforward manner. These studies suggest that this simplified approach could be very useful as a tool for future PDE design and optimization.

Acknowledgments

This work has been supported at University of California, Los Angeles, by NASA Dryden Flight Research Center under Grant NCC4-153 with Trong Bui and Dave Lux as technical monitors, and by the Office of Naval Research under Grants ONR 00014-97-0027 and ONR N00014-03-1-0071, with Wen Masters as technical monitor. The authors wish to thank Fred Schauer and Leonard Shaw of the Air Force Research Laboratory Propulsion Directorate for sharing data regarding pulse-detonation-engine sound pressure levels.

References

[1]Eidelman, S., Grossmann, W., and Lottati, I., "Review of Propulsion Applications and Numerical Simulations of the Pulse Detonation Engine Concept," *Journal of Propulsion and Power*, Vol. 7, No. 6, 1991, pp. 857–865.

[2]Kailasnath, K., "Review of Propulsion Applications of Detonation Waves," *AIAA Journal*, Vol. 38, No. 9, 2000, pp. 1698–1708.

[3]Kailasanath, K., "Recent Developments in the Research on Pulse Detonation Engines," *AIAA Journal*, Vol. 41, No. 2, 2003, pp. 145–159.

[4]Kailasanath, K., "A Review of PDE Research—Performance Estimates," AIAA Paper 2001-0474, Jan. 2001.

[5]Kailasanath, K., and Patnaik, G., "Performance Estimates of Pulse Detonation Engines," *Proceedings of the Combustion Institute*, Vol. 28, 2000, pp. 595–602.

[6]Cambier, J.-L., and Tegner, J. K., "Strategies for Pulse Detonation Engine Performance Optimization," *Journal of Propulsion and Power*, Vol. 14, No. 4, 1998, pp. 489–498.

[7]Wintenberger, E., Austin, J. M., Cooper, M., Jackson, S., and Shepherd, J. E., "An Analytical Model for the Impulse of a Single Cycle Pulse Detonation Engine," *Journal of Propulsion and Power*, Vol. 19, No. 4, 2003, pp. 22–38; also *Journal of Propulsion and Power*, Vol. 20, No. 4, 2004, pp. 765–767.

[8]Ebrahimi, H. B., and Merkle, C. L., "Numerical Simulation of a Pulse Detonation Engine with Hydrogen Fuels," *Journal of Propulsion and Power*, Vol. 18, No. 5, 2002, pp. 1042–1048.

[9]Mattison, D. W., Brophy, C. M., Sanders, S. T., Ma, L., Hinckley, K. M., Jeffries, J. B., and Hanson, R. K., "Pulse Detonation Engine Characterization and Control Using Tunable Diode-Laser Sensors," *Journal of Propulsion and Power*, Vol. 19, No. 4, 2003, pp. 568–572.

[10]Morris, C. I., "Numerical Modeling of Single-Pulse Gasdynamics and Performance of Pulse Detonation Rocket Engines," *Journal of Propulsion and Power*, Vol. 21, No. 3, 2005, pp. 527–538

[11]Johnson, C., "The Effects of Nozzle Geometry on the Specific Impulse of a Pulse Detonation Engine," Massachusetts Inst. of Technology, Final Report 16.622, Cambridge, MA, Dec. 2001.

[12]Cooper, M., and Shepherd, J. E., "The Effect of Nozzles and Extensions on Detonation Tube Performance," AIAA Paper 02-3628, July 2002.

[13]Kennedy, J. E., "The Gurney Model of Explosive Output for Driving Metal," *Explosive Effects and Applications*, edited by J. S. Zuker and W. P. Walters, Springer-Verlag, New York, 1998, pp. 221–257, Chap. 7.

[14]Yungster, S., "Analysis of Nozzle and Ejector Effects on Pulse Detonation Engine Performance," AIAA Paper 2003-1316, Jan. 2003.

[15]Hwang, P., Fedkiw, R., Merriman, B., Karagozian, A. R., and Osher, S. J., "Numerical Resolution of Pulsating Detonation Waves," *Combustion Theory and Modeling*, Vol. 4, No. 3, 2000, pp. 217–240.

[16]He, X., and Karagozian, A. R., "Numerical Simulation of Pulse Detonation Engine Phenomena," *Journal of Scientific Computing*, Vol. 19, No. 1–3, 2003, pp. 201–224.

[17]He, X., "Numerical Simulation of Pulse Detonation Engine Flow Processes," Ph.D. Dissertation, Dept. of Mechanical and Aerospace Engineering, Univ. of California, Los Angeles, June 2004.

[18]Kee, R. J., Miller, J. A., and Jefferson, T. H., "CHEMKIN: A General Purpose, Problem Independent, Transportable, Fortran Chemical Kinetics Code Package," Sandia National Lab., Rept. SAND80-8003, Livermore, CA, 1980.

[19]Ma, F., Choi, J. Y., and Yang, V., "Thrust Chamber Dynamics and Propulsive Performance of Single-Tube Pulse Detonation Engines," *Journal of Propulsion and Power*, Vol. 21, No. 3, 2005, pp. 512–526.

[20]Ma, F., Wu, Y., Choi, J.-Y., and Yang, V., "Thrust Chamber Dynamics and Propulsive Performance of Multi-Tube Pulse Detonation Engines," *Journal of Propulsion and Power*, Vol. 21, No. 4, 2005, pp. 681–691.

[21]Shu, C. W., and Osher, S., "Efficient Implementation of Essentially Non-Oscillatory Schock Capturing Schemes II," *Journal of Computational Physics*, Vol. 83, No. 1, 1989, pp. 32–78.

[22]Jiang, G. S., and Shu, C. W., "Efficent Implementation of Weighted ENO Schemes," *Journal of Computational Physics*, Vol. 126, No. 1, 1996, pp. 202–228.

[23]Henrick, A. K., Aslam, T. D., and Powers, J. M., "Mapped Weighted Essentially Non-oscillatory Schemes: Achieving Optimal Order near Critical Points," *Journal of Computational Physics*, Vol. 207, No. 2, 2005, pp. 542–567.

[24]Strikwerda, J. C., *Finite Difference Schemes and Partial Differential Equations*, Wadsworth and Brooks, Monterey, CA, 1989.

[25]Brown, P. N., Byrne, G. D., and Hindmarsh, A. C., "VODE: A Variable Coefficient ODE Solver," *SIAM Journal of Scientific Statistical Computing*, Vol. 10, No. 5, 1989, pp. 1038–1051.

[26]Lee, J. H. S., "Initiation of Gaseous Detonation," *Annual Review of Physical Chemistry*, Vol. 28, 1977, pp. 74–104.

[27]Sileem, A. A., Kassoy, D. R., and Hayashi, A. K., "Thermally Initiated Detonation Through Deflagration to Detonation Transition," *Proceedings of the Royal Society of London A: Mathematical and Physical Sciences*, Vol. 435, No. 1895, 1991, pp. 459–482.

[28]Lighthill, M. J., "On Sound Generated Aerodynamically: I. General Theory," *Proceedings of the Royal Society of London, Series A: Mathematical and Physical Sciences*, Vol. 211, 1952, pp. 564–587.

[29]Eldredge, J., "A Dilating Vortex Particle Method for Compressible Flow with Applications to Aeroacoustics," Ph.D. Dissertation, Mechanical Engineering, California Inst. of Technology, Pasadena, June 2001.

[30]Li, C., and Kailasanath, K., "Partial Fuel Filling in Pulse Detonation Engines," *Journal of Propulsion and Power*, Vol. 19, No. 5, 2003, pp. 908–916.

[31]Benedick, W. B., Guirao, C. M., Knystautas, R., and Lee, J. H., "Critical Charge for the Direct Initiation of Detonation in Gaseous Fuel-Air Mixtures," *Progress in Astronautics and Aeronautics*, Vol. 106, 1986, pp. 181–202.

[32]Zitoun, R., and Desbordes, D., "Propulsive Performances of Pulsed Detonations," *Combustion Science and Technology*, Vol. 144, Nos. 1–6, 1999, pp. 93–114.

[33]Schauer, F., Stutrud, J., and Bradley, R., "Detonation Initiation Studies and Performance Results for Pulsed Detonation Engines," AIAA Paper 2001-1129, Jan. 2001.

[34]Shaw, L., Harris, K., Schauer, F., and Hoke, J., "Acoustics Measurements for a Pulse Detonation Engine," AIAA Paper 2005-2952, May 2005.

[35]Lele, S. K., and Colonius, T., "Computational Aeroacoustics: A Review of Numerical Approaches and Progress in Nonlinear Problems of Sound Generation," *Progress in Aerospace Sciences*, Vol. 40, No. 6, 2004, pp. 345–416.

[36]Goodman, J., "Convective Instability of Hollow Sedov-Taylor Blast Waves," *The Astrophysical Journal*, Vol. 358, No. 1, Part 1, 1990, pp. 214–228.

[37]Falempin, F., Bouchaud, D., and Forrat, B., "Pulse Detonation Engine: Possible Application to Low Cost Tactical Missile and to Space Launcher," AIAA Paper 2001-3815, 2001.